STIS Instrument Science Report 97-09

The STScI STIS Pipeline: Bias Level Correction

Paul Goudfrooij and Jeremy R. Walsh
May 1997

ABSTRACT

The properties of the bias frame of the STIS SITe 1024x1024 CCD, including its serial and parallel overscan regions, are described. Overscan regions are listed for all supported binning factors. There are significant differences in the (2-D) behavior of the bias level in the sensitive region of the STIS CCD with respect to that found in the serial and parallel overscan regions, resulting in the necessity of an additional 2-D zero level correction. Flat fields taken with the (operational) amplifier D show an amplifier non-linearity: the bias level of a given row is found to be dependent on the signal in that row. Analysis of the right-hand side overscan region of flat field images shows that the bias value is ***depressed*** *with respect to the nominal bias value by an amount proportional to the mean signal in the row. The dependence on signal level depends on the binning in the X direction of the CCD. The maximum dependence is found in the case of unbinned data, where the overscan bias level is depressed by 1 electron per (average) row signal of roughly 1380 electrons. For the majority of science observations, we recommend to perform overscan subtraction by a smooth, low-order fit to the bias level in the left-hand serial overscan. Such a fit will be insensitive to the "depression problem", since only a few rows will be affected in case of scientific observations. Observers will be able to estimate the effect of the "depression problem" from the parallel (virtual) overscan in raw, full-frame CCD images.*

1. The STIS SITe CCD: Overscan Regions

The STIS SITe CCD has pixel dimensions 1024 by 1024. All pixel coordinates given in this ISR refer to the coordinate system of *raw (unprocessed)* in-flight images[1]. In addition to the sensitive pixels of the CCD, there are four overscan regions: columns at the the left- and right-hand edges of the CCD represent physical serial overscan, and rows at the

1. The coordinates of the in-flight data have been flipped along both axes with respect to the pre-flight data. The pre-flight data which are used in this report have been converted to the in-flight coordinate system.

top- and bottom edges represent virtual parallel overscan. The top-edge overscan region consists of only one row in unbinned images, and is thus of no particular use. The number of columns/rows in the overscan regions depends on the binning factor employed. Table 1 lists the "safe" overscan regions for all available binning factors. This excludes pixels with "mixed" information (overscan + sensitive) as well as the last few pixels along each row which exhibit a significant "roll-off" in the bias value (cf. Figure 1). The most usable overscan regions are (i) the one on the left-hand edge of the chip (serial overscan) and (ii) the one on the bottom edge of the chip (virtual overscan).

Figure 1: Trace of the mean DN level for bias frame taken in `CCDGAIN=1`, showing the roll-off at the right edge of the CCD. 1000 rows were averaged together.

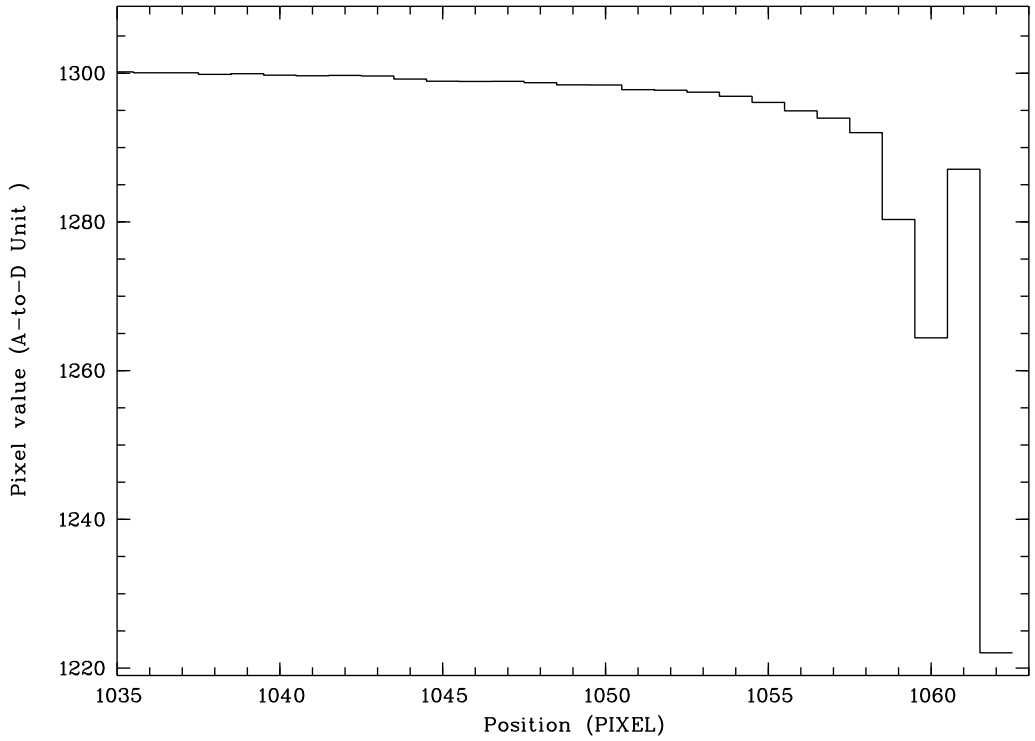

Table 1. Total image sizes (FITS keywords `SIZEAXIS1` and `SIZEAXIS2`) and "safe" overscan regions for the available binning factors All numbers are in CCD pixels. A question mark indicates that it is difficult to determine a overscan region free of sensitive pixels or roll-off to the edge of the chip.

Bin Mode	Image Size	Left Overscan	Right Overscan	Bottom Overscan
1x1	1062x1044	2 - 16	1045 - 1057	1 - 12
1x2	1054x522	2 - 8	1037 - 1049	1 - 9

Bin Mode	Image Size	Left Overscan	Right Overscan	Bottom Overscan
1x4	1054x266	2 - 8	1037 - 1049	1 - 9
2x1	532x1034	2 - 8	525 - 529	1 - 9
4x1	271x1034	2 - 8	268 - 270 (?)	1 - 9
2x2	532x522	2 - 8	525 - 529	1 - 9
4x2	271x522	2 - 8	268 - 270 (?)	1 - 9
2x4	532x266	2 - 8	525 - 529	1 - 9
4x4	271x266	2 - 8	268 - 270 (?)	1 - 9

2. Behavior of data in the overscan regions

2.1. Consistency of slopes along rows and columns of overscan regions

Using bias frames taken during Ground Calibration at GSFC, the consistency of the behavior of the overscan regions of the CCD has been investigated. Results are shown in Figures 2 - 4 for the serial overscan region on the left-hand edge of the chip (all "safe" columns were averaged) and in Figures 5 - 7 for the parallel overscan region on the bottom edge of the chip (all "safe" rows were averaged). As depicted in these Figures, the behavior of the overscan regions is very stable from one bias frame to another. Typically, the RMS difference among second-order polynomial fits to overscan vectors for a given `CCD-GAIN` setting stays within 0.1 DN. Quantitative information on the stability is given below in Table 2 for all supported modes of operation.

Table 2. Parameters for second-order polynomial fits (`BIAS = A + Bf + Cf`^{2}, where `f` = `AXIS1` for the BOTTOM overscan and `f` = `AXIS2` for the LEFT overscan) for the parallel (BOTTOM) and serial (LEFT) overscan regions of the chip, for all supported gain settings. The mean R.M.S. error of the fits and their standard deviations are also tabulated.

Overscan / Gain	A	B	C	RMS
BOTTOM / 1	1300.6 +/- 0.6	(-0.08 +/- 0.12) 10^{-2}	(+0.16 +/- 0.92) 10^{-6}	0.13 +/- 0.04
BOTTOM/ 2	1438.3 +/- 0.6	(+0.14 +/- 0.03) 10^{-1}	(-0.34 +/- 0.05) 10^{-4}	0.17 +/- 0.02
BOTTOM/ 4	1498.0 +/- 0.2	(-0.75 +/- 0.24) 10^{-3}	(-0.17 +/- 0.24) 10^{-6}	0.17 +/- 0.01
LEFT/ 1	1300.7 +/- 0.4	(+0.02 +/- 0.45) 10^{-3}	(-0.11 +/- 0.41) 10^{-6}	0.10 +/- 0.01
LEFT/ 2	1421.1 +/- 0.5	(+0.31 +/- 0.86) 10^{-3}	(-0.02 +/- 0.14) 10^{-5}	0.10 +/- 0.01
LEFT/ 4	1494.3 +/- 0.1	(+0.09 +/- 0.76) 10^{-3}	(-0.02 +/- 0.14) 10^{-5}	0.06 +/- 0.01

Figure 2: Traces of the mean overscan level along columns of the left-hand overscan region of 21 selected unbinned bias frames taken in `CCDGAIN=1` mode. All "safe" rows of the overscan region were averaged. To recognize the traces of the different individual bias frames, each has been shifted up by an amount slightly greater than the noise in the overscan level, as well as assigned a different greyscale.

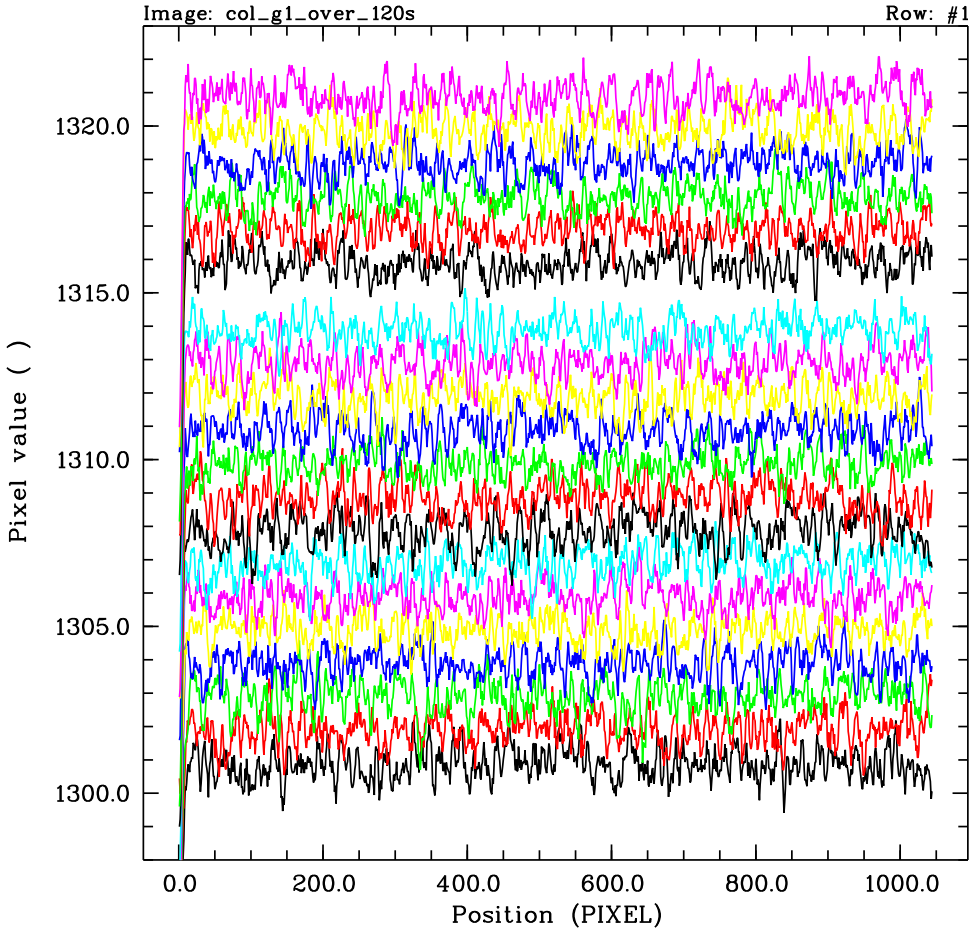

Figure 3: As Figure 2, for 10 selected bias frames taken in `CCDGAIN=2` mode.

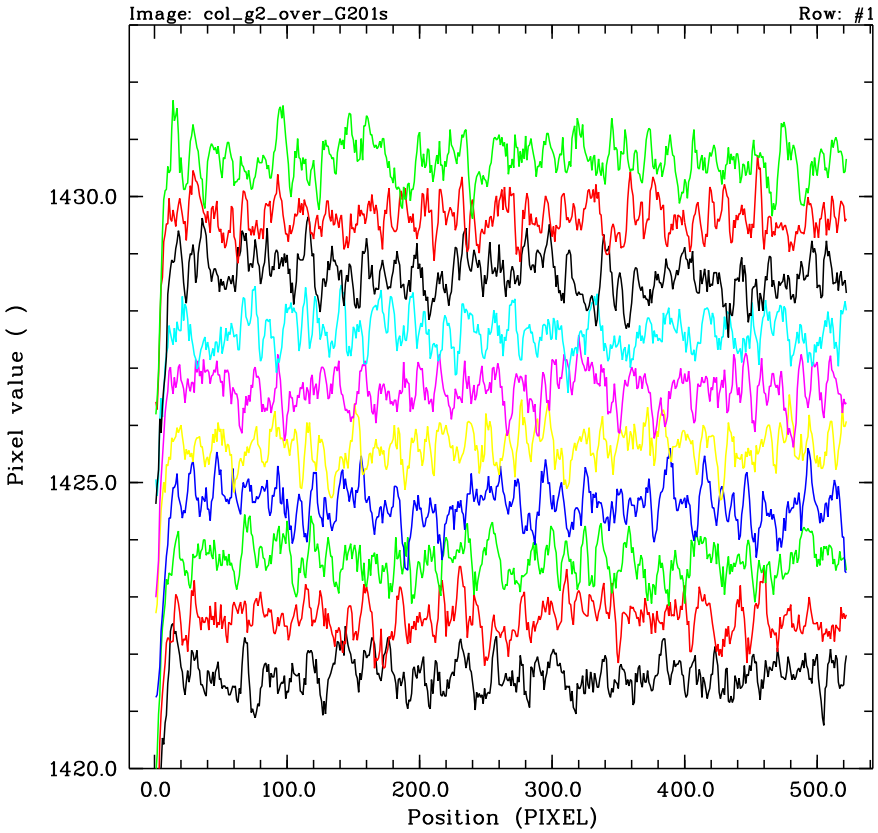

Figure 4: As Figure 2, for 11 selected bias frames taken in `CCDGAIN=4` mode.

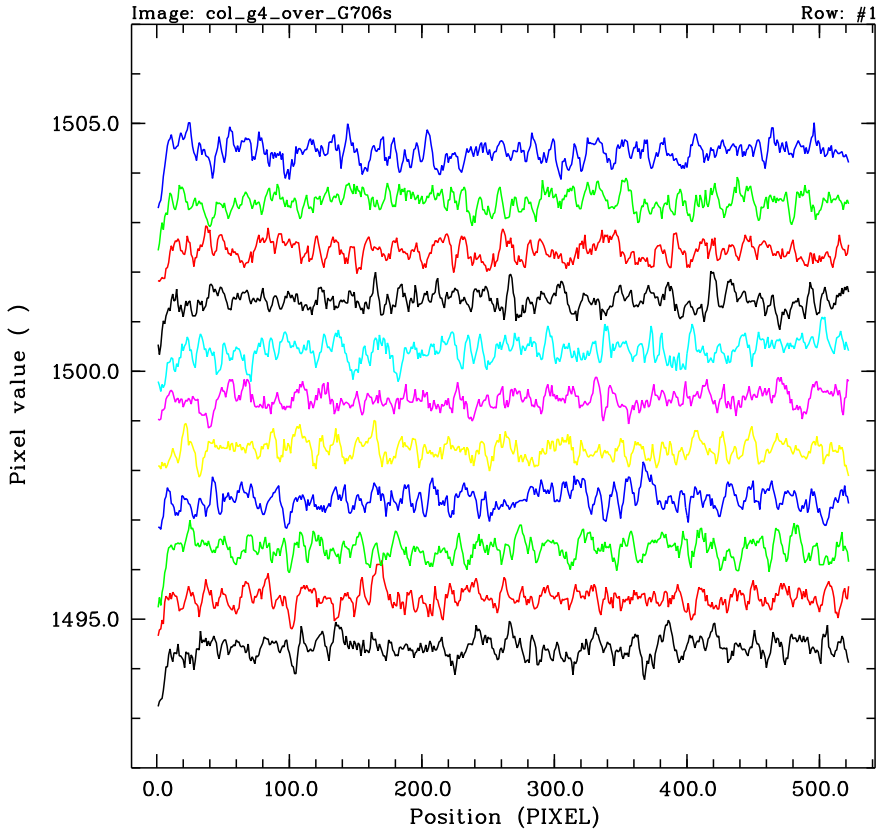

Figure 5: Traces of the mean overscan level along rows of the overscan region at the bottom edge of the chip of 21 selected unbinned bias frames taken in `CCDGAIN=1` mode. All "safe" columns of the overscan region were averaged. To recognize the traces of the different individual bias frames, each has been shifted up by an amount slightly greater than the noise in the overscan level, as well as assigned a different greyscale.

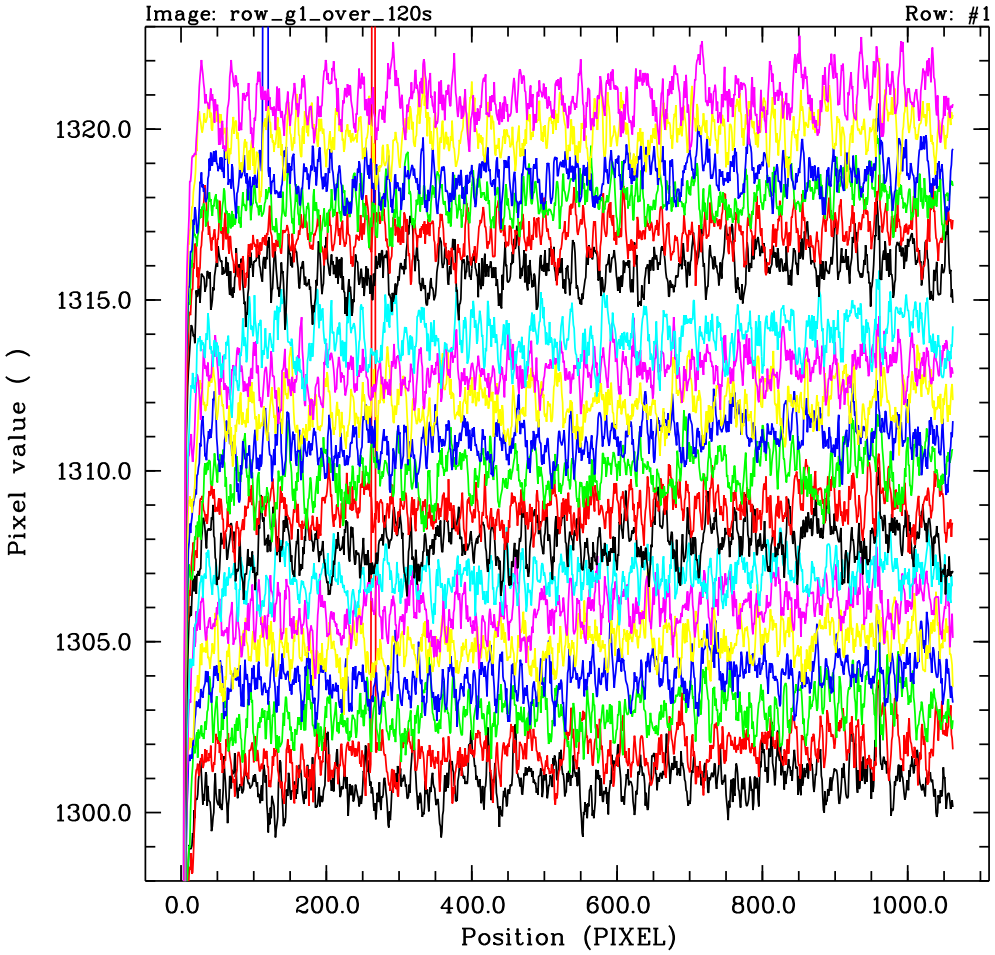

Figure 6: As Figure 5, for 10 selected bias frames taken in `CCDGAIN=2` mode.

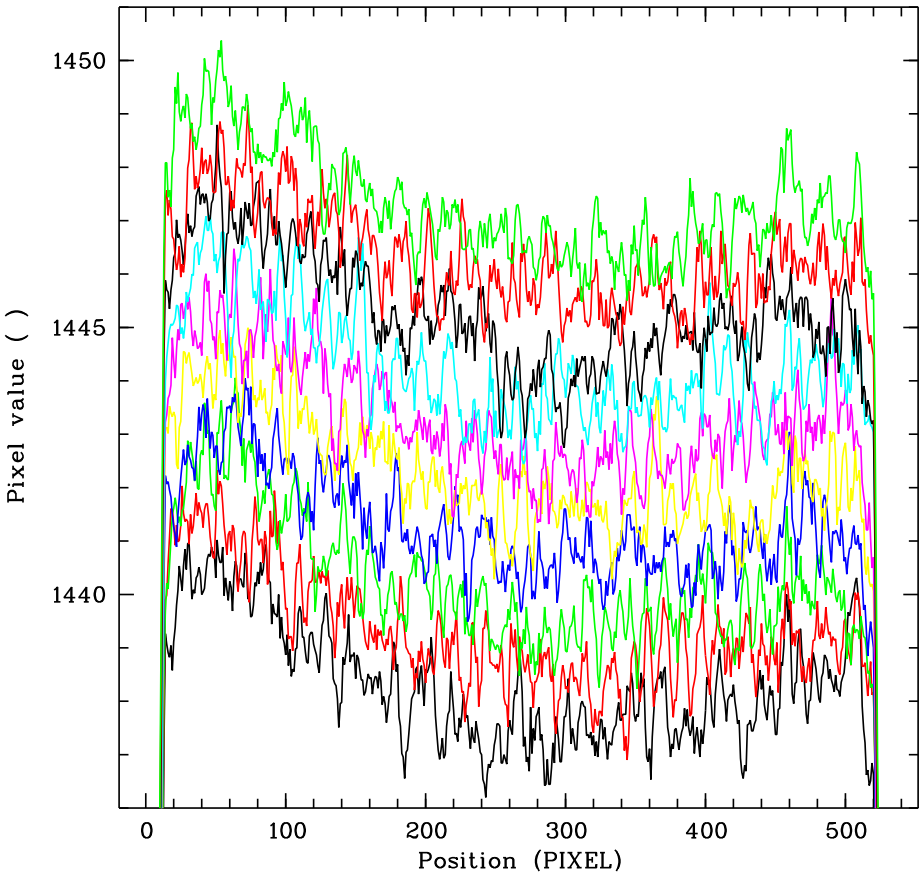

Figure 7: As Figure 5, for 11 selected bias frames taken in CCDGAIN=4 mode.

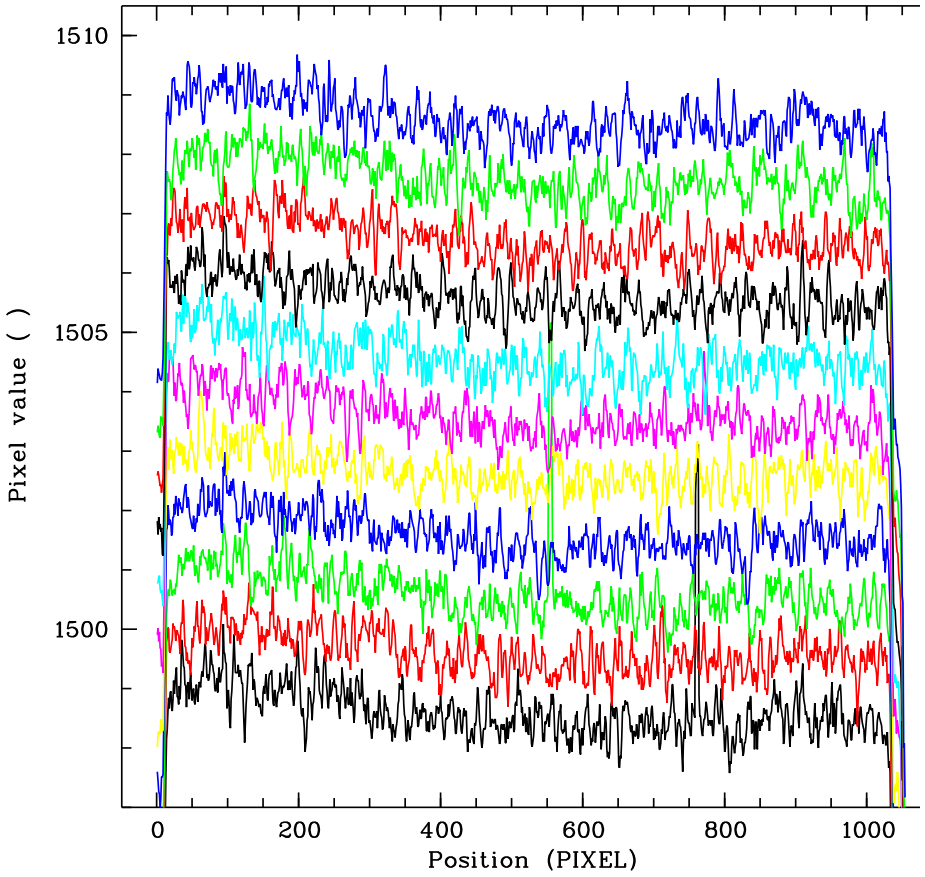

2.2. Amplifier non-linearity feature revealed through level of serial overscan regions

Analysis of CCD images taken during Ground Calibration has revealed the existence of a non-linearity of the operational amplifier D: the bias level of a given row is found to be dependent on the signal in that row. Analysis of the serial overscan regions of flat field images shows that the bias value is actually *depressed* with respect to the nominal bias value by an amount proportional to the mean signal in the row (cf. Figure 8). This shows up most clearly in highly illuminated flat field images taken in spectroscopic mode, where the serial overscan shows depressed ADU values except for the rows in which the fiducial bars of STIS are located (see Figure 9). The dependence on signal depends on the binning in the X direction of the CCD. Least-square fits to flat field images covering a suitable range in illumination levels have shown the dependences of the depression level on the mean signal in a row given in Table 3. The proportionality factors mentioned in this table are for the CCDGAIN=1 amplifier setting; for the CCDGAIN=2 and CCDGAIN=4 settings, they are smaller by the respective factors.

Figure 8: Trace across left-hand overscan region of highly illuminated CCD flatfield image `fsw15639.fits`. This particular image was binned 1x2, and illuminated only in rows 131 - 380 (i.e., using a 25 arcsec aperture). The “safe” columns of the overscan region were averaged together. Note the depression of the bias level in the overscan at the illuminated rows.

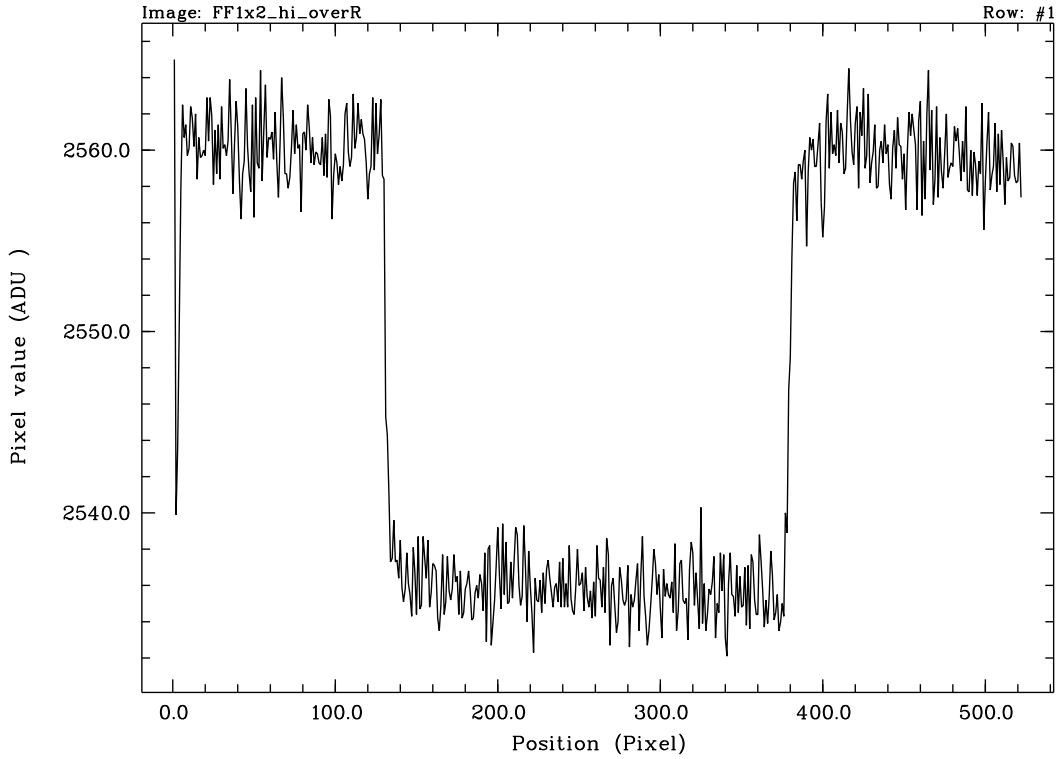

Figure 9: Screendump of SAOimage displaying the top right area of a highly-illuminated flatfield image taken in spectroscopy mode. ***NOTE OF CAUTION: THIS IMAGE IS PRE-FLIGHT, I.E., FLIPPED ALONG BOTH AXES.*** Notice the depression of the bias level in the overscan region near the right-hand edge of the CCD, except in the rows covering the location of the upper fiducial occulting bar of the STIS spectrograph (the approximately correct bias level is that reached in the overscan region near the top edge).

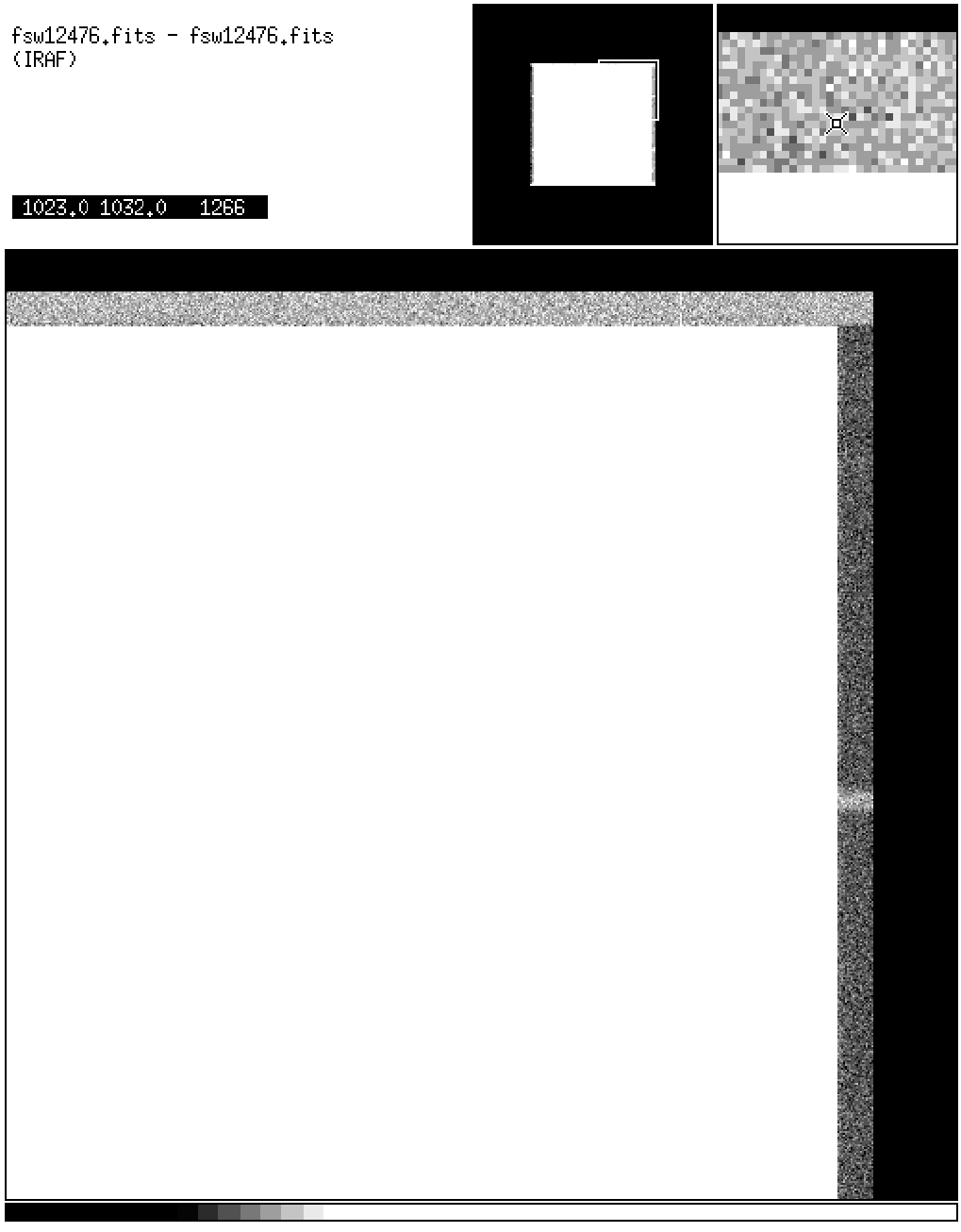

Table 3. Dependence of the depression level on the average signal in a row*. The proportionality factors mentioned in this table are for the `CCDGAIN=1` amplifier setting; for the `CCDGAIN=2` and `CCDGAIN=4` settings, they are smaller by the respective factors.

Binning Factor in X	Proportionality Factor
1	$(7.25 +/- 0.41)\ 10^{-4}$
2	$(3.49 +/- 0.20)\ 10^{-4}$
4	$(4.14 +/- 0.42)\ 10^{-5}$

* NOTE: The "average" signal refers here to the average of *the illuminated part of the CCD*, rather than the average across the whole row (the data used for this study had a flat field illumination covering the middle third of the `AXIS1` direction of the CCD); a steeper dependence is found if the strict average across the whole row is used for the fit to these data. A somewhat shallower dependence was found for another (unbinned) dataset of flat field images in which the whole CCD was illuminated, *suggesting that it is not only the average signal across the row but also the variation of signal with position within a row* which affects the observed depression in the bias level.

2.3. Cause and effect of "depression problem"

The current view upon the cause of this feature is that the problem occurs whenever there is a sudden increase in intensity encountered during readout. Thus, scientific data will be affected by this problem (this has indeed been confirmed in Ground Calibration data). However, the small proportionality factors at which the nonlinearity occurs (cf. Table 3; e.g., for unbinned data this means a bias depression of 1 electron per (average) row signal of roughly 1380 electrons) render the problem negligible regarding the majority of scientific applications of STIS. Instances of science that may be slightly influenced by this problem are: (1) aperture photometry of faint sources (in imaging mode), especially in case of a crowded region with nearby bright sources which would cause a local depression of the bias value, (2) photometry of diffuse extended objects which cover a large number of pixels. In the case of spectroscopy, the presence of a very strong emission line will cause a local depression in the nearby continuum (since the dispersion direction is along the rows of the CCD), which will limit the sensitivity to search for weak line wings to those having > 0.1% of the peak intensity of that line.

2.4. Discussion: Implications for data reduction procedures

The "depression problem" mentioned above will influence scientific data obtained with the STIS CCD to some level, so that special care in deciding how to perform bias level subtraction is in order.

The parallel (virtual) overscan is *not* subject to this amplifier non-linearity problem. Although it would then seem best to use the parallel overscan for bias level subtraction,

this would be imprudent since one would not be able to allow for the development of a slope along the columns of the bias frames (i.e., the read-out direction).

Another sensible method of bias level subtraction would be to determine the bias level on a row-by-row basis, since one would then subtract the appropriate bias level for each row (independent on the depression level for any particular row). However, only a few columns are averaged in this case to determine the bias level, so that the r.m.s. noise on the average bias for a single row will not be insignificant (e.g., > 5 electrons in the case of unbinned data, less for data binned in `AXIS2`). As only a minority of STIS data will be significantly affected by the "depression problem", we do not recommend this method to be used *in general* (e.g., in the context of pipeline reduction). However, observers concerned about the effect of the "depression problem" to their data might consider performing bias level subtraction on a row-by-row basis.

As to the usual method of bias level subtraction (using the serial overscan), we note that only relatively few rows of the CCD will be significantly impacted for the majority of imaging and spectroscopic data. Thus, a smooth, low-order fit to the bias in the serial overscan will not be influenced if appropriate kappa-sigma clipping (to exclude deviant data points in the fit) is performed. *In the context of the STIS pipeline module `calstis-1` (see Hodge & Baum 1995), we therefore recommend to use a smooth, low-order fit to the bias in the left-hand serial overscan (see above) for bias level subtraction*[2]. Obviously, this procedure will produce erroneous results for the case of flat field images, as the whole left-hand serial overscan will suffer from the "depression problem" in that case. *Therefore we recommend to take separate bias frames before and after flat field images to perform bias level correction for flat field images.*

Observers will be able to estimate the effect of the "depression problem" from the parallel (virtual) overscan in raw, full-frame CCD images. Note that *observers using subarrays* (e.g., to reduce the time interval between reads and limit the data volume when performing variability observations in the optical [see e.g., Chapter 11 of Baum et al., "STIS Instrument Handbook", version 1.0]) *will obtain only the serial overscan.* Thus, in case the whole sub-array is filled by a strong source spectrum, an estimate of the depression in the serial overscan will *not* be possible.

3. The need for 2-D zero level correction

There are significant differences in the (2-D) behavior of the bias level in the sensitive region of the STIS CCD with respect to that found in the serial and parallel overscan regions, resulting in the necessity of an additional 2-D zero level correction. The level of significance is different for the different gain settings. Details are mentioned below.

---

2. By the time this report is issued, `calstis-1` has been modified accordingly.

3.1. Comparison between slopes along rows and columns of overscan- and sensitive regions

The sensitive region of several bias frames have been collapsed along rows and columns to compare the behavior of these traces with those of the overscan regions. These comparisons are depicted in Figures 10 - 15. These Figures show the following trends:

1. The behavior along the CCD columns of the serial overscan is *not* the same as that along the columns of the sensitive region of the CCD. The sensitive region suffers from accumulative *spurious charge* which starts to accumulate at row #512 (in unbinned images). This effect is most dramatic in the `CCDGAIN=2` setting, where the spurious charge reaches 17.5 ADU over 512 (unbinned) pixels. In the case of the `CCDGAIN=4` setting, the spurious charge reaches 4.5 ADU over 512 (unbinned) pixels, but in the `CCDGAIN=1` setting it reaches a mere 0.45 ADU over 512 (unbinned) pixels.
2. The behavior along CCD rows of the parallel overscan is consistent with that along rows of the sensitive region of the CCD. This holds for all `CCDGAIN` settings.

In view of trend 1) above, it is not sufficient to perform bias correction using the overscan region(s) only; an additional 2-D zero level correction is necessary. This holds for all supported `CCDGAIN` settings and binning factors.

Figure 10: Comparison of the trace along columns within the serial (left-hand) overscan region (bottom trace) with the trace along columns of the sensitive region (top trace) of an unbinned bias frame taken in `CCDGAIN=1`.

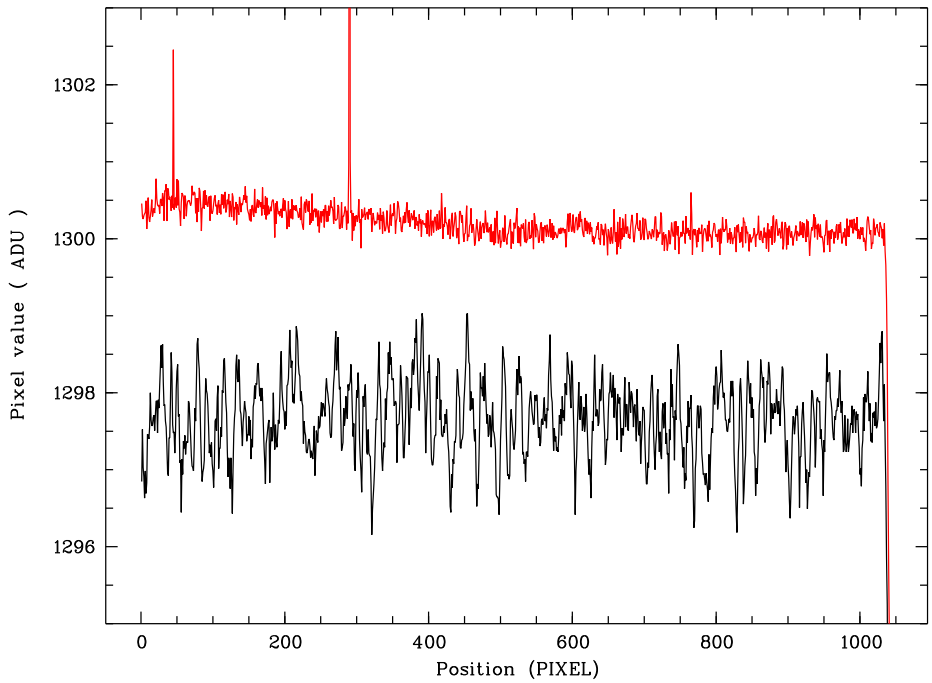

Figure 11: As Figure 10, for a bias frame taken in `CCDGAIN=2`, binned 2x2.

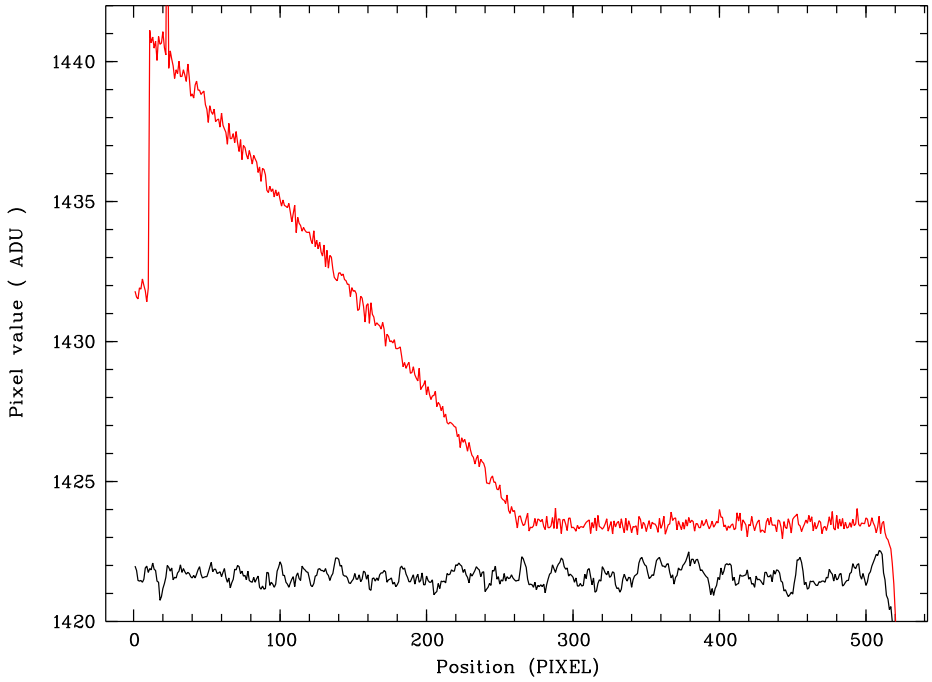

Figure 12: As Figure 10, for a bias frame taken in `CCDGAIN=4`, binned 1x2.

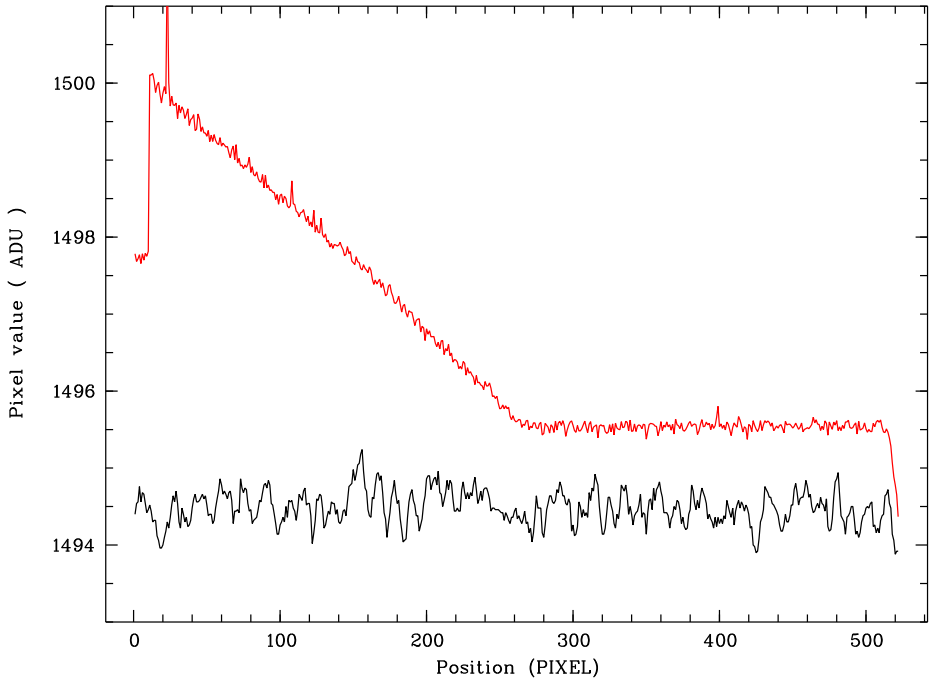

Figure 13: Comparison of the trace along rows within the parallel (bottom) overscan region (bottom trace) with the trace along rows of the sensitive region (top trace) of an unbinned bias frame taken in `CCDGAIN=1`.

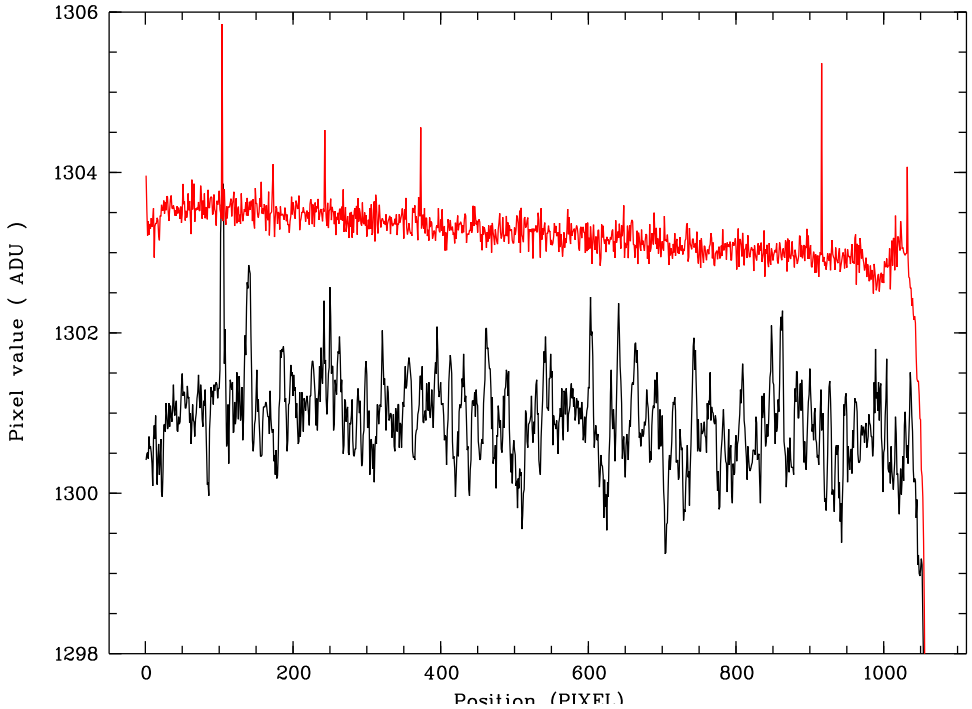

Figure 14: As Figure 13, for a bias frame taken in `CCDGAIN=2`, binned 2x2.

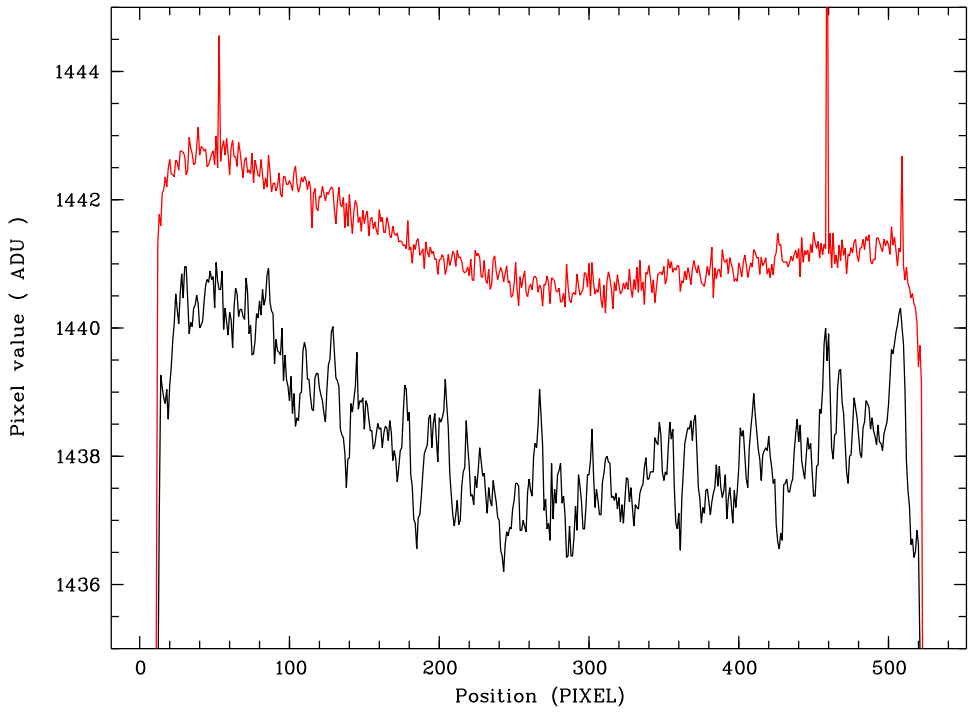

Figure 15: As Figure 13, for a bias frame taken in `CCDGAIN=4,` binned 1x2.

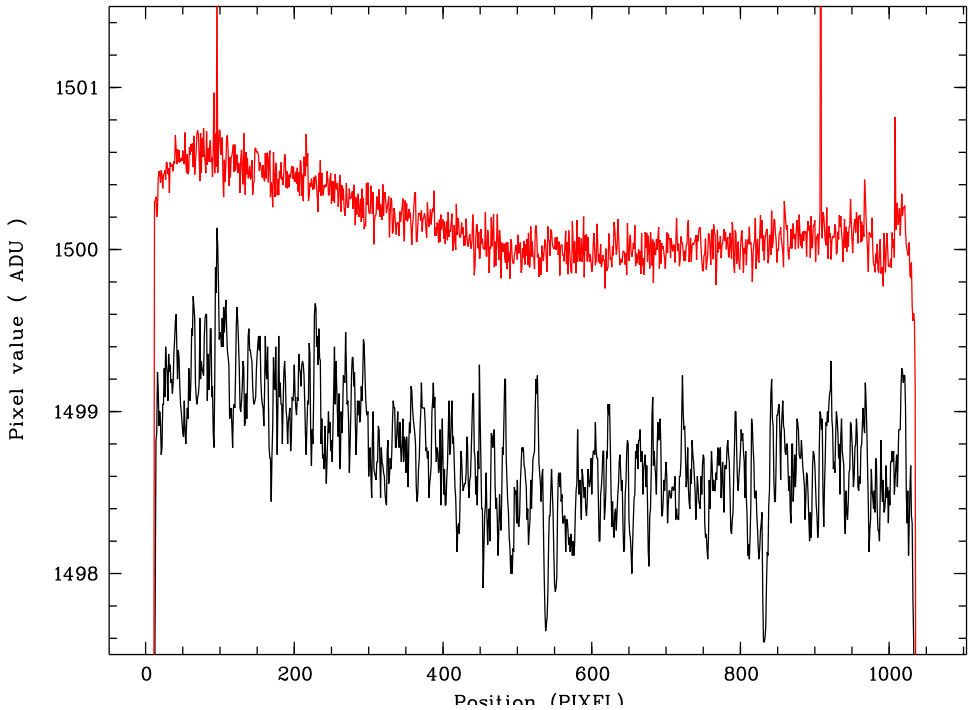

4. Analysis of the stability of the 2-D shape of the bias pattern

Several bias frames from the IDT archive at GSFC (taken during different sessions) have been analyzed to study the stability of the shape of the bias pattern over time. Subarrays of 80 x 80 pixels were investigated, positioned at regular intervals on the CCD. Each subarray was designated a local overscan level being the average value over 80 rows in the serial overscan region (after kappa-sigma clipping of the deviant values). After subtraction of the local overscan value, the “residuals” in the different subarrays were compared with one another. Sample residual-residual plots are shown in Figures 16 - 18. No correlations were found. The overall R.M.S. noise in the residuals was < 0.2 ADU.

References

1. Phil Hodge & Stefi Baum, 1995, STIS Instrument Science Report 95-007.

Figure 16: Residual signal (after subtraction of local overscan level) in two 80 x 80 pixel subarrays plotted against one another, for a collection of bias frames taken during different sessions of Ground Calibration. Frames were taken in `GAIN=1` for this example.

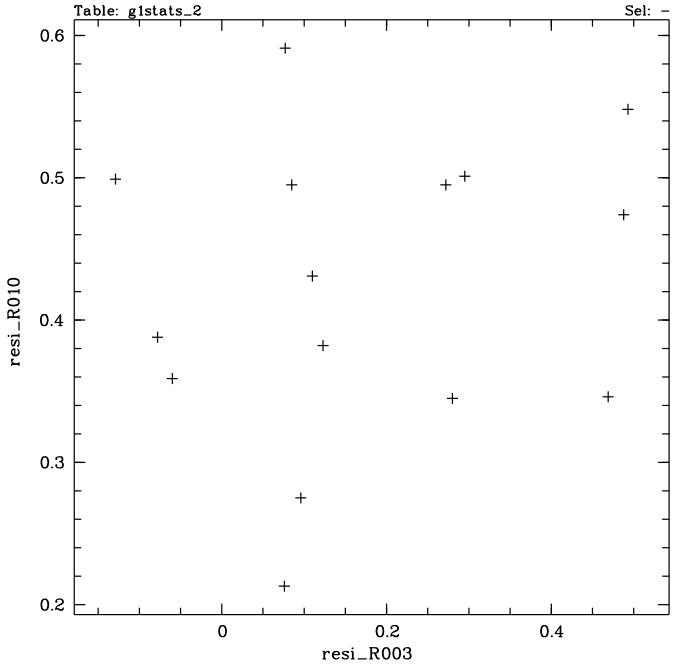

Figure 17: As Fig. 16, for two 80 x 80 pixel subarrays, displaced from those in Fig. 16.

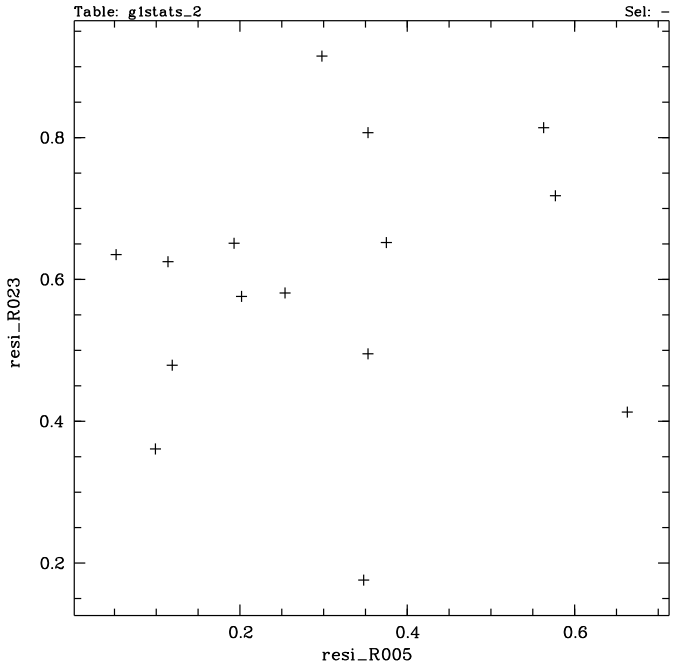

Figure 18: As Fig. 16, again for two different 80 x 80 pixel subarrays.